Tunable graphene-based polarizer

Yu. V. Bludov,[1, a)] M. I. Vasilevskiy,[1] and N. M. R. Peres[1]
Centro de Física & Departamento de Física, Universidade do Minho, Campus de Gualtar, Braga 4710-057, Portugal

It is shown that an attenuated total reflection structure containing a graphene layer can operate as a tunable polarizer of the electromagnetic radiation. The polarization of the reflected electromagnetic wave is controlled by adjusting the voltage applied to graphene via external gate, as demonstrated for the cases of linearly and circularly polarized incident radiation. The mechanism is based on the resonant coupling of $p-$polarized waves to the surface plasmon-polaritons in graphene. The presented calculations show that, at resonance, the reflected wave is almost 100% $s-$polarized.

I. INTRODUCTION

Surface plasmon-polaritons (SPPs) are excitations of electromagnetic (EM) radiation coupled to surface charges existing at a metal-dielectric interface.[1,2] Under certain conditions, they can interact with external EM waves giving rise to a number of optical effects ranging from resonant absorption and enhanced non-linearities to surface-enhanced Raman scattering.[3] The potential applications of SPPs in detection, signal processing and information transfer originated the appearance of a new and rapidly growing research area called plasmonics.[3,4]

Graphene, a monolayer thick metal is attracting much attention in different areas[5–7] due to its unique and unusual physical properties. For plasmonics, the interest in graphene stems from the possibility of controlling the charge carrier density through electrostatic "doping" using an external gate voltage.[8,9] As a consequence, the spectrum of SPPs in graphene is tunable as it is determined by the optical conductivity that depends on the free carrier concentration.[10] This idea is supported by the observation of plasmon absorption bands in monolayer and multilayer graphene sheets[11] and in graphene ribbons.[12] The demonstration of a tunable terahertz (THz) source,[13] is another plasmonic-based application of graphene. These applications open the possibility of building graphene-based metamaterials and new optoelectronic devices, such as a THz detector,[12] a broad band modulator,[14] an optical switch,[15] and an enhanced platform for radiation absorption in the terahertz and infrared spectral ranges.[16,17] Increasing the electron density by charge doping[18] can make these devices work also in the infrared domain.

The EM response of graphene is characterized by its optical conductivity that can be written as $\sigma(\omega) = \sigma' + i\sigma''$, where σ' and σ'' are real functions of frequency, ω. A unique property of doped graphene is that the imaginary part of the conductivity, σ'', can be either positive or negative depending on the frequency and the electronic chemical potential, μ. The conductivity is determined by both intraband scattering (Drude term) and interband transitions, and reaches a (negative value) minimum at $\hbar\omega \approx 2\mu$.[10] As a consequence, and in contrast with usual metals, graphene can support either transverse magnetic (TM) or transverse electric (TE) surface waves, depending on whether σ'' is positive or negative.[19] The existence of TE-type (or $s-$polarized) SPPs is unique to graphene and has been demonstrated experimentally.[20] Let us note at this point that their dispersion relation is quite different from that of "conventional" TM-type (or $p-$polarized) SPPs, as it will be further discussed below.

Conventional polarizers use one of the following operation principles: (i) polarization-dependent absorption in anisotropic media, (ii) refraction by a prism, and (iii) polarization by reflection at Brewster angle.[21] Recently, the idea of filtering of one of the polarizations using a graphene-based device has been proposed and it allowed for demonstration of a polarizer that can operate in the infrared range.[20] The device consisted of an optical fiber some part of which was side-polished and cladded with a graphene sheet. Due to the higher attenuation of the $p-$component of the EM field (if the radiation is in resonance with TE plasmon-polaritons), a rather high degree of the TM component filtering could be achieved, given the graphene-cladded segment of the fiber is long enough (though, the TE component is attenuated, too). We propose another possible operation principle for a graphene based polarizer, making use of the resonant coupling of the external EM radiation to SPPs in an attenuated total reflection (ATR) structure considered in our previous work[15] and schematically shown in Fig. 1.

In this paper we demonstrate the possibility of polarization of unpolarized incoming EM radiation by its reflection in an ATR graphene-based structure. The degree of polarization can be controlled by varying the external gate voltage applied to graphene. Circularly polarized radiation can be transformed into linearly polarized one and *vice versa*. In other words, we will show that such a graphene-based ATR structure can operate as a tunable polarizer of the EM radiation. At the resonant frequency, that depends on the gate voltage, the $p-$component of the incident wave is almost 100% filtered out.

II. REFLECTIVITY OF ATR STRUCTURE

Let us consider the ATR scheme for coupling SPPs to an external EM wave using so called Otto configuration[2] (see Fig. 1). In this configuration, a linearly polarized EM wave with frequency ω impinges on the interface between the prism, with a dielectric constant ε_3, and a graphene layer sandwiched between a substrate (with a dielectric constant ε_1) and a capping layer (with a dielectric constant ε_2). We assume that all these dielectric constants are real. If the angle of incidence Θ is larger than the critical angle of total internal reflection Θ_c

a)Electronic mail: bludov@fisica.uminho.pt

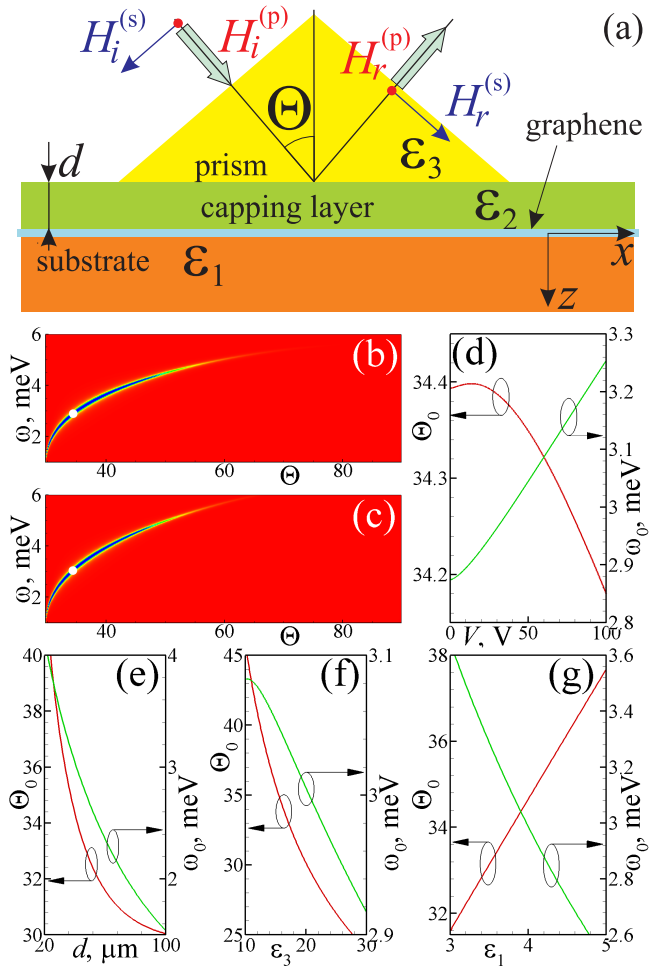

FIG. 1. (a) ATR structure in Otto configuration, containing a graphene layer on the substrate, and a prism separated from graphene by a capping layer of thickness d; (b, c) Reflectivity $R = \left|H_r^{(p)}\right|^2$ versus angle of incidence Θ, and frequency ω for the ATR structure with $\mu \simeq 0.1\,\text{eV}$ (b), or $\mu \simeq 0.222\,\text{eV}$ (c) [corresponding to $V = 10\,\text{V}$ and $50\,\text{V}$ of gate voltage, respectively], where blue (red) color corresponds to low (high) reflectivity; (d-g) Angle of incidence Θ_0, and frequency ω_0, corresponding to zero reflectivity of the ATR structure versus gate voltage V (d), capping layer thickness d (e), dielectric constant of prism ε_3 (f) or substrate ε_1 (g). Other parameters are: $\varepsilon_1 = 3.9$ (panels b–f), $\varepsilon_2 = 1$ (panels b–g), $\varepsilon_3 = 16$ (panels b–e, g), $d = 40\,\mu\text{m}$ (panels b–d, f, g), $V = 50\,\text{V}$ (panels e–g) and $\varphi = 90^\circ$ ($p-$polarized wave). In panels (b, c) white circles depict pairs of parameters (Θ_0, ω_0) corresponding (in each case) to zero reflectivity.

[determined by the relation $\sin^2\Theta_c = \max(\varepsilon_1, \varepsilon_2)/\varepsilon_3$], then the EM wave in the gap between the prism and graphene will be evanescent in the z direction. The same is true for the field in the substrate ($z > 0$).

Two situations, qualitatively different in terms of coupling of the external EM wave to SPPs in graphene, are possible: (i) if the x-component of the incident wave vector, $k_x = (\omega/c)\sqrt{\varepsilon_3}\sin\Theta$, does not match $k_{SPP}(\omega)$, the SPP wave vector in graphene, there is virtually no interaction between them and the incident wave is almost totally reflected at the prism-capping layer interface (the reflectivity is close to unity); (ii) if $k_x \simeq k_{SPP}(\omega)$, the incident EM wave and the polariton mode are in resonance and the impinging energy is transferred to the excitated SPPs in graphene resulting in a drastic decrease of the reflectivity. The operation mechanism of the polarizer is now easy to understand. Assuming that the frequency of the impinging radiation lies in the spectral region where $\sigma'' > 0$, $p-$polarized SPPs can be induced in graphene. A linear polarized wave with an arbitrary polarization orientation can be represented as a sum of TE and TM waves without phase shift. If the wave is in resonance with SPP, the $p-$polarized component of the *reflected* wave is strongly attenuated whereas the $s-$polarized one has almost the same amplitude as in the incident wave. This leads to a rotation of the polarization plane of the reflected EM wave with respect to that of the impinging radiation.

In order to describe the proposed mechanism quantitatively, we solve Maxwell's equations, $\text{rot}\mathbf{E}^{(m)} = i\kappa\mathbf{H}^{(m)}$, $\text{rot}\mathbf{H}^{(m)} = -i\kappa\varepsilon_m\mathbf{E}^{(m)}$, separately for each of three media ($m = 1, 2, 3$). Since the system is uniform in the y direction, we can decompose the electromagnetic fields $\mathbf{E}^{(m)}$, $\mathbf{H}^{(m)}$ into two components and consider the s and $p-$polarized waves separately. For the latter, the magnetic field vector is perpendicular to the plane of incidence (xz) and we have $\mathbf{H}^{(m)} = \{0,\, H_y^{(m)},\, 0\}$ and $\mathbf{E}^{(m)} = \{E_x^{(m)},\, 0,\, E_z^{(m)}\}$. For the $s-$polarized wave, the magnetic field vector lies in the plane of incidence, $\mathbf{H}^{(m)} = \{H_x^{(m)},\, 0,\, H_z^{(m)}\}$) and $\mathbf{E}^{(m)} = \{0,\, E_y^{(m)},\, 0\}$. The amplitudes of p and $s-$polarized parts of the incident wave are $H_i^{(p)} = H_i\sin\varphi$, and $H_i^{(s)} = H_i\cos\varphi$, where φ denotes the angle between the plane of incidence and the direction of the magnetic field.

In the semi-infinite medium 3 (representing the prism and occupying the half-space $z < -d$) the solution of Maxwell's equations reads:

$$H_x^{(3)}(x,z) = -\exp(ik_x x)\cos\Theta \times \{H_i\exp[ik_z(z+d)]\cos\varphi - H_r^{(s)}\exp[-ik_z(z+d)]\}, \quad (1)$$

$$E_y^{(3)}(x,y) = \frac{1}{\sqrt{\varepsilon_3}\sin\Theta}H_z^{(3)} = \exp(ik_x x)\frac{1}{\sqrt{\varepsilon_3}} \times \{H_i\exp[ik_z(z+d)]\cos\varphi + H_r^{(s)}\exp[-ik_z(z+d)]\}, \quad (2)$$

for the $s-$polarized wave, and

$$H_y^{(3)}(x,z) = -\frac{\sqrt{\varepsilon_3}}{\sin\Theta}E_z^{(3)}(x,z) = \exp(ik_x x) \times \{H_i\exp[ik_z(z+d)+i\delta]\sin\varphi + H_r^{(p)}\exp[-ik_z(z+d)]\}, \quad (3)$$

$$E_x^{(3)}(x,z) = \exp(ik_x x)\frac{\cos\Theta}{\sqrt{\varepsilon_3}} \times \{H_i\exp[ik_z(z+d)+i\delta]\sin\varphi - H_r^{(p)}\exp[-ik_z(z+d)]\}, \quad (4)$$

for the $p-$polarized one. We have defined $k_z = \kappa\sqrt{\varepsilon_3}\cos\Theta$ as the z-component of the wave vector, $\kappa = \omega/c$, and δ is a phase shift between the p and $s-$polarized waves. Note that two limiting cases, $\varphi = 0$ and $\varphi = \pi/2$, correspond to purely s and $p-$polarized incident waves, respectively. In this cases, the reflected wave is linear polarized. Other values of

φ and δ imply linear (when $\delta = 0$), circular (when $\delta = \pi/2$, $\varphi = \pi/4$), or elliptic (all other cases) polarization of the incident wave. Notice that for arbitrary φ and δ the (complex) amplitudes of the p and $s-$polarized reflected waves, $H_r^{(p)}$ and $H_r^{(s)}$, do not have the same phase. In general, this phase difference gives rise to an elliptic polarization of the reflected wave.

In the dielectric film between the prism and graphene ($-d < z < 0$, medium $m = 2$), and in the substrate below graphene ($z > 0$, medium $m = 1$) the solution of Maxwell's equations is:

$$H_x^{(m)}(x,z) = \exp(ik_x x) \times \left\{A_+^{(m)} \exp[p_m z] + A_-^{(m)} \exp[-p_m z]\right\}, \quad (5)$$

$$E_y^{(m)}(x,y) = \frac{1}{\sqrt{\varepsilon_3}\sin\Theta} H_z^{(m)} = -\exp(ik_x x)\frac{i\kappa}{p_m} \times \left\{A_+^{(m)} \exp[p_m z] - A_-^{(m)} \exp[-p_m z]\right\}, \quad (6)$$

for the $s-$polarized wave, and

$$H_y^{(m)}(x,z) = -\frac{\varepsilon_m}{\sqrt{\varepsilon_3}\sin\Theta} E_z^{(m)}(x,z) = \exp(ik_x x) \times \left\{B_+^{(m)} \exp[p_m z] + B_-^{(m)} \exp[-p_m z]\right\}, \quad (7)$$

$$E_x^{(2)}(x,z) = -i\frac{p_m}{\kappa\varepsilon_m} \exp(ik_x x) \times \left\{B_+^{(m)} \exp[p_m z] - B_-^{(m)} \exp[-p_m z]\right\}, \quad (8)$$

for the $p-$polarized one. The fields are represented in the form of evanescent waves [in Eqs. (5) - (8) $p_m = \kappa\sqrt{\varepsilon_3 \sin^2\Theta - \varepsilon_m} \geq 0$]. The case $m = 2$ corresponds to a superposition of two evanescent waves, while for $m = 1$ we must have $A_+^{(1)} = B_+^{(1)} = 0$, that is, the solution represents a single wave of the amplitude exponentially decreasing with the distance z to graphene.

The boundary conditions at $z = -d$ and $z = 0$ are different. At the prism-dielectric interface, $z = -d$, they imply the continuity of the tangential components of the electric and magnetic fields, $E_{x,y}^{(3)}(x,-d) = E_{x,y}^{(2)}(x,-d)$, $H_{x,y}^{(3)}(x,-d) = H_{x,y}^{(2)}(x,-d)$]. At the interface $z = 0$ the condition is different due to the presence of the conductive graphene layer. In this case, we have the continuity of the tangential components of the electric field, $E_{x,y}^{(1)}(x,0) = E_{x,y}^{(2)}(x,0)$, whereas the tangential component of the magnetic field is discontinuous, that is, we have $H_y^{(1)}(x,0) - H_y^{(2)}(x,0) = -(4\pi/c)j_x = -(4\pi/c)\sigma(\omega)E_x(x,0)$, $H_x^{(1)}(x,0) - H_x^{(2)}(x,0) = (4\pi/c)j_y = (4\pi/c)\sigma(\omega)E_y(x,0)$. Matching these boundary conditions, we obtain explicit expressions for the amplitudes of the reflected fields,

$$H_r^{(s)} = H_i \cos\varphi \frac{\left\{p_1 - i\frac{4\pi\kappa}{c}\sigma(\omega)\right\}\overline{\eta_1} + p_2\overline{\eta_2}}{\left\{p_1 - i\frac{4\pi\kappa}{c}\sigma(\omega)\right\}\eta_1 + p_2\eta_2}, \quad (9)$$

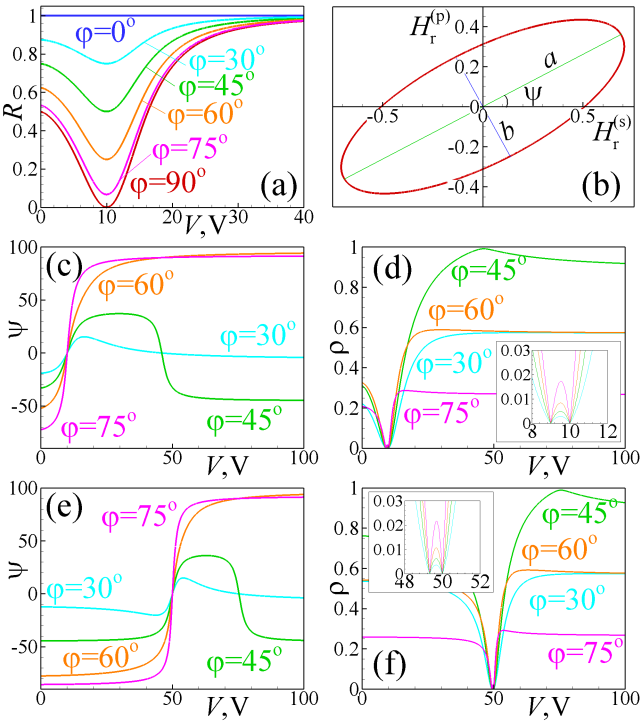

FIG. 2. (a) Reflectivity $R = \left|H_r^{(p)}\right|^2 + \left|H_r^{(s)}\right|^2$ of EM waves with different polarization angles φ (as indicated on the plot) *versus* gate voltage; (b) Vibrational ellipse of the magnetic field vector in the reflected wave for $V = 15$ V; (c, d, e, f) Dependence of the orientation angle of the ellipse, ψ (c, e) and the ellipticity, ρ (d, f) upon the applied gate voltage for different polarization angles of the linear polarized incident wave (as indicated on the plot) and $\Theta = 34.40\,^\circ$, $\hbar\omega = 2.894$ meV (c, d) or $\Theta = 34.35\,^\circ$, $\hbar\omega = 3.044$ meV (e, f). Other parameters of the ATR structure are the same as in Fig. 1. The insets in (d, f) show zoom into the region near the minimum of ρ.

for the $s-$polarized component, and

$$H_r^{(p)} = -H_i \sin\varphi e^{i\delta} \frac{\left\{\frac{\varepsilon_1}{p_1} + i\frac{4\pi}{c\kappa}\sigma(\omega)\right\}\overline{\chi_1} + \frac{\varepsilon_2}{p_2}\overline{\chi_2}}{\left\{\frac{\varepsilon_1}{p_1} + i\frac{4\pi}{c\kappa}\sigma(\omega)\right\}\chi_1 + \frac{\varepsilon_2}{p_2}\chi_2}, \quad (10)$$

for the $p-$polarized one, where we have defined

$$\eta_1 = \tanh[p_2 d] + \frac{ip_2}{\kappa\sqrt{\varepsilon_3}\cos\Theta},$$

$$\eta_2 = 1 + \frac{ip_2}{\kappa\sqrt{\varepsilon_3}\cos\Theta}\tanh[p_2 d],$$

$$\chi_1 = \tanh[p_2 d] - \frac{i\kappa\varepsilon_2\cos\Theta}{p_2\sqrt{\varepsilon_3}},$$

$$\chi_2 = 1 - \frac{i\kappa\varepsilon_2\cos\Theta}{p_2\sqrt{\varepsilon_3}}\tanh[p_2 d],$$

and the bars over $\eta_{1,2}$ and $\chi_{1,2}$ denote complex conjugates.

III. RESULTS AND DISCUSSION

Let us analyze the properties of Eqs. (9)–(10). We note that in the limit of an infinitely thick layer separating the prism and graphene, $d \to \infty$, the denominator of Eq. (9) is equal to zero if

$$p_1 + p_2 - i\frac{4\pi\kappa}{c}\sigma(\omega) = 0, \qquad (11)$$

while for Eq. (10) the same condition yields,

$$\frac{\varepsilon_1}{p_1} + \frac{\varepsilon_2}{p_2} + i\frac{4\pi}{c\kappa}\sigma(\omega) = 0. \qquad (12)$$

Substitution of $k_{SPP} = \kappa\sqrt{\varepsilon_3}\sin\Theta$ into Eqs. (11) and (12) transforms them into the dispersion relations, $\omega(k_{SPP})$, for TE [Eq. (11)], and TM [Eq. (12)] surface waves in graphene cladded by two semi-infinite media with dielectric constants ε_1 and ε_2. Despite some algebraic similarity between these relations, the p and $s-$ polarized SPPs possess quite different properties. As mentioned above, Eq. (12) has solution, i.e. $p-$polarized SPPs exist if $\sigma'' > 0$, whereas solution of Eq. (11) ($s-$polarized surface wave) exists in the opposite case. Taking into account the form of the optical conductivity of graphene[8,10], we conclude that the two types of waves exist in different spectral ranges, namely, $p-$polarized SPPs are present at low frequencies ($\hbar\omega < 2\mu$), while $s-$polarized waves exist at frequencies in the vicinity of $\hbar\omega \sim 2\mu$; the chemical potential depends on the gate voltage as $\mu \sim \sqrt{V}$.

Since the working principle of the polarizer is based on the excitation of TM SPPs, in Figs. 1(b-d) we present the $p-$polarized reflectance spectra in detail. As discussed above, resonant excitation of SPPs for a frequency ω is manifested by the appearance of a reflectivity minimum [Figs. 1(b,c)] at a certain angle Θ. Excitation of SPPs in graphene is characterized by two interesting properties. First, the position of the resonant reflectivity minimum can be tuned by changing the gate voltage applied to the graphene layer, as it follows from the comparison of Figs. 1(b) and 1(c). Secondly, if the incident wave is purely $p-$polarized ($\varphi = 90°$), and for any given value of the gate voltage (and other parameters), it is possible to find a pair of values, (Θ_0, ω_0), for which the reflectivity of the ATR structure is zero. In Figs. 1(b,c) these pairs are depicted by white circles. Below, the pair (Θ_0, ω_0) for a given V is referred to as *zero-point*. In other words, at the zero-point the whole energy of the incident wave is transformed into energy of excited SPPs. In Figs. 1(d)– 1(g) the pair (Θ_0, ω_0) is shown as a function of the gate voltage [Fig. 1(d)], capping layer thickness [Fig. 1(e)], dielectric constant of prism [Fig. 1(f)], and substrate [Fig.1(g)].

How does the tunable polarizer work? If the parameters V , Θ, and ω are chosen is such a way that $\Theta = \Theta_0$ and $\omega = \omega_0$ for the given V, and the incident wave is not purely $p-$polarized, ($\varphi \neq 90°$), then its $p-$polarized part is completely absorbed, while the $s-$polarized part is almost totally reflected, giving rise to the total reflectivity $R \approx \cos^2\varphi$ [see Fig. 2(a)]. In this case we have pure $s-$polarization of the reflected EM radiation with a single passage through the device.

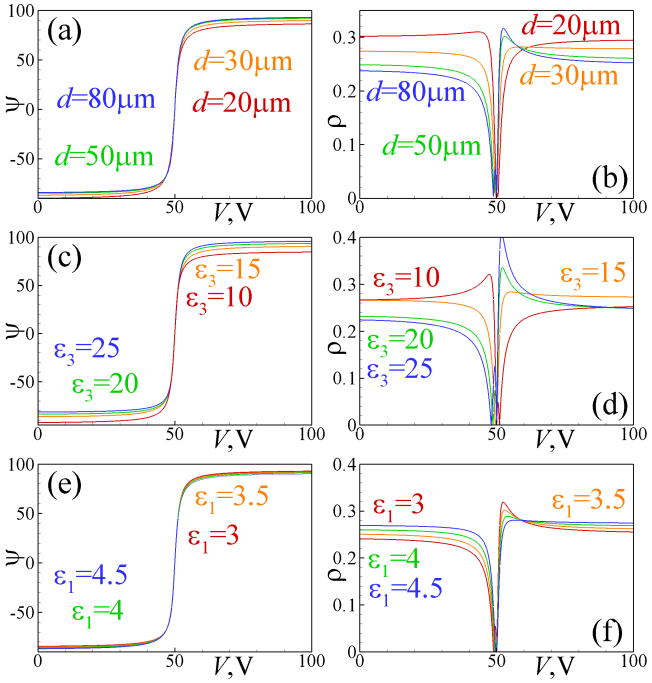

FIG. 3. Dependence of the orientation angle of the ellipse, ψ (a, c, e) and the ellipticity, ρ (b, d, f) upon the applied gate voltage for the polarization angle $\varphi = 75^o$ and different values of the capping layer thickness d (a, b), and dielectric constant of the prism ε_3 (c, d) and the substrate ε_1 (e, f), as indicated in the plot. Other parameters of the ATR structure for each plot are the same as in Fig.1. The angle of incidence Θ and frequency ω are different for different curves in each plot. For panels (a, b), (c, d), and (e, f) they can be determined from Figs. 1(e), 1(f), and 1(g), respectively.

Keeping unchanged Θ and ω, and slightly detuning V from its initial value deviates the system from the condition necessary for the full absorption of the $p-$polarized component. The reflected wave then should contain the fully reflected $s-$polarized component as well as a small $p-$polarized part. Therefore, the total reflectivity R increases [Fig. 2(a)] and, in general, the reflected light will be elliptically polarized [an example is shown in Fig. 2(b)]. Further detuning of the gate voltage will result in a further increase of the total reflectivity and the corresponding decrease of the polarization ratio.

In what follows we want to characterize the reflected wave in more detail, namely, to investigate the shape and orientation of the vibrational ellipse characterized by the orientation angle ψ and the ellipticity $\rho = b/a$[22] [see Fig. 2(b) for definitions of these quantities] as function of the gate voltage. Figs. 2(c-f) summarize our results for linearly polarized incident wave ($\delta = 0$). At the zero-point, pure $s-$polarization of the reflected wave corresponds to $\psi = 0$ [Figs. 2(c) and 2(e)] and zero ellipticity [Figs. 2(d) and 2(f)]. In its vicinity, an increase of the gate voltage results in an anti-clockwise rotation of the vibrational ellipse, since ψ increases as seen in Figs. 2(c) and 2(d). Far from the zero-point, the increase of ψ is monotonic for $\varphi > 45°$ and has a maximum at a certain V for $\varphi \leq 45°$. When the gate voltage V is detuned from the zero-point, the reflected wave ellipticity ρ becomes non-zero.

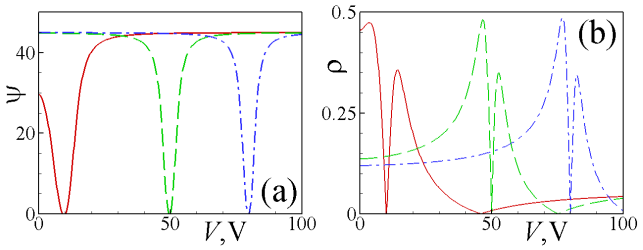

FIG. 4. Dependence of the orientation angle of the ellipse, ψ (a) and the ellipticity, ρ (b) upon the applied gate voltage for circular polarization of incident wave and $\Theta = 34.40\,^\circ$, $\hbar\omega = 2.894\,\mathrm{meV}$ (solid red line), $\Theta = 34.35\,^\circ$, $\hbar\omega = 3.044\,\mathrm{meV}$ (dashed green line), and $\Theta = 34.26\,^\circ$, $\hbar\omega = 3.17\,\mathrm{meV}$ (dash-and-dotted blue line). Other parameters of the ATR structure are the same as in Fig. 1.

However, as it follows from the insets of Figs. 2(d) and 2(f), in the vicinity of the zero point there is another value of V, $V \approx 9\,\mathrm{V}$ in Fig. 2(d) and $V \approx 49.3\,\mathrm{V}$ in Fig. 2(f), at which the reflected wave is linearly polarized ($\rho = 0$). Although this point bears some similarity with the zero-point, the reason for $\rho = 0$ is different. Here the linear polarization of the reflected wave stems from the phase shift (equal to π) between the s and $p-$components, while at the zero-point it is due to the full absorption of its $p-$component. We also notice that a steeper variation of ψ with V, close to the zero point, occurs for larger values of φ. The same happens for the ellipticity ρ. For $\varphi \lesssim 90°$, ρ is close to zero (linear polarization). Therefore, for these angles of polarization of the incident wave. the reflected radiation presents a large ψ and a small ellipticity for V slightly detuned from the zero point. Finally, we point out that for $\varphi = 45^o$ it is possible to obtain nearly circularly polarized reflected radiation ($\rho = 1$) at some particular values of gate voltage [$V = 46.25\,\mathrm{V}$ in Fig. 2(d) and $V = 75.6\,\mathrm{V}$ in Fig. 2(f)].

Another important question is the following: how sensitive is the polarization of the reflected EM wave to the parameters of the polarizer? The answer to this question follows from Fig. 3. For a typical fixed polarization angle of $\varphi = 75^o$, the dependence of $\psi(V)$ on the capping layer thickness d [Fig. 3(a)], dielectric constant of the prism ε_3 [Fig. 3(c)] and the substrate [Fig. 3(e)] is very small. On the other hand, the ellipticity ρ is more sensitive to the above-mentioned parameters. In short, the ellipticity of the reflected EM wave decreases with the increase of both the capping layer thickness d [Fig. 3(b)] and the prism dielectric constant ε_3 [Fig. 3(d)], and with the decrease of the substrate dielectric constant ε_1 [Fig. 3(f)]. It is worth noticing two points. First, in Fig. 3 the dependencies are calculated for lossless dielectrics (when the losses are taken into account, the results can be slightly different). Secondly, the angle of incidence (Θ) and the frequency (ω) are *not* kept constant for different curves $\psi(V)$ and $\rho(V)$; for each value of d [in Figs. 3(a),3(b)], of ε_3 [in Figs. 3(c), 3(d)], and of ε_1 [in Figs. 3(e), 3(f)] the pair (Θ, ω) is taken in order to achieve the zero-point at gate voltage $V = 50\,\mathrm{V}$.

For a circularly polarized incident wave ($\delta = \pi/2$, $\varphi = \pi/4$), the situation is somewhat different (Fig. 4). In this case, *any* detuning of gate voltage V from the zero-point results in an anti-clockwise rotation (positive ψ) of the vibrational ellipse [see Fig. 4(a)]. Exactly at the zero-point, the reflected wave is still purely $s-$polarized, with $\psi = \rho = 0$. Similarly to the previous case [see Figs. 2(d) and 2(f)], the phase shift between the s and $p-$components of the reflected wave is equal to π for some particular values of the gate voltage [$V = 46\,\mathrm{V}$ for the solid red curve and $V = 75\,\mathrm{V}$ for the dashed green curve in Fig. 4(b)], that gives rise to the linear polarization of the reflected wave ($\rho = 0$).

IV. SUMMARY

To conclude, we have demonstrated that an ATR structure containing a single graphene layer can work as a tunable polarizer of the EM radiation in the THz frequency domain, in a broad range of gate voltages. Although we have considered the case where the incident radiation is linearly or circularly polarized, it is possible to generalize our results to the case of elliptic polarization. The nearly complete absorption of the TM component of unpolarized incident radiation at resonance will yield a high polarization ratio of the reflected waves. Also, we would like to point out the possibility of using the same principle for filtering out $s-$polarized component of the incident wave. It would allow to extend the operation frequency range to the infrared domain. However, our calculations show that, in general, the resonance with TE polaritons in graphene is weaker than with $p-$polarized SPPs.

ACKNOWLEDGMENT

We acknowledge financial suport from FEDER-COMPETE, and from the Portuguese Foundation for Science and Technology (FCT) through grant PEst-C/FIS/UI0607/2011.

[1] A. A. Maradudin, Surface Polaritons. Electromagnetic Waves at Surfaces and Interfaces, ed V. M. Agranovich and D. L. Mills, Amsterdam, North-Holland, 1982.
[2] J. Zhang, L. Zhang, and W. Xu, J. Phys. D: Appl. Phys. 45, 113001 (2012).
[3] M. I. Stockman, Phys. Today 64, 39 (2011).
[4] S. Maier, *Plasmonics: Fundamentals and Applications*, Springer, 2007.
[5] A. K. Geim and K. S. Novoselov, Nature Materials 6, 183 (2007).
[6] A. K. Geim, Science 324, 1530 (2009).
[7] M. J. Allen, V. C. Tung and R. B. Kaner, Chem. Rev. 110, 132 (2010).
[8] Z. Q. Li, E. A. Henriksen, Z. Jiang, Z. Hao, M. C. Martin, P. Kim, H. L. Stormer, and D. N. Basov, Nature Phys. 4, 532 (2008).
[9] V. Ryzhii, A. Satou, and T. Otsuji, J. Appl. Phys. 101, 024509 (2007)
[10] N. M. R. Peres, Rev. Mod. Phys. 82, 2673 (2010).
[11] Omer Salihoglu, Sinan Balci, and Coskun Kocabas, Appl. Phys. Lett. 100, 213110 (2012).
[12] L. Ju, B. Geng, J. Horng, C. Girit, M. C. Martin, Z. Hao, H. A. Bechtel, X. Liang, A. Zettl, Y. Ron Shen, and F. Wang, Nature Nanotechnol. 6, 630 (2011).
[13] V. Ryzhii, M. Ryzhii, and T. Otsuji, J. Appl. Phys. 101, 083114 (2007); F. Rana, IEEE Trans. NanoTechnol. 7, 91 (2008).
[14] M. Liu, X. Yin, E. Ulin-Avila, B. Geng, T. Zentgraf, L. Ju, F. Wang, and X. Zhang, Nature 474, 64 (2011).
[15] Yu. V. Bludov, M. I. Vasilevskiy, and N. M. R. Peres, Europhys. Lett. 92, 68001 (2010).
[16] N. M. R. Peres, A. Ferreira, Yu. V. Bludov, and M. I. Vasilevskiy, J. Phys.: Condens. Matter **24**, 245303 (2012).

[17] Yu. V. Bludov, N. M. R. Peres, and M. I. Vasilevskiy, Phys. Rev. B **85**, 245409 (2012)
[18] S. Y. Shin *et.al,*, Appl. Phys. Lett. 99, 082110 (2011).
[19] S. A. Mikhailov and K. Ziegler, Phys. Rev. Lett. 99, 016803 (2007).
[20] Qiaoliang Bao, Han Zhang, Bing Wang, Zhenhua Ni, Candy Haley Yi Xuan Lim, Yu Wang, Ding Yuan Tang, and Kian Ping Loh, Nature Phot. 5, 411 (2011).
[21] D. Goldstein, *Polarized Light*, Marcel Dekker Inc., New York, 2003.
[22] M. Born and E. Wolf, *Principles of Optics*, Pergamon, Oxford, 1989.